Synthesis of MgO nanostructure thin films via electrodeposition method for gas sensing applications

N. Lal[1,3], A. Kumar[2], K. Chawla[1,4], S. Sharma[1,5] and C. Lal[1,2]*

[1]*Department of Physics, University of Rajasthan, Jaipur, Rajasthan 302004, India*

[2]*Centre for Non-Conventional Energy Resources, University of Rajasthan, Rajasthan 302004, India*

[3]*Govt. Girls College, Jhunjhunu, Rajasthan 333001, India*

[4]*Govt. College, Pratapgarh, Rajasthan 312605, India*

[5]*Govt. College, Jhunjhunu, Rajasthan 333001, India*

Abstract

Magnesium oxide has long been intriguing due to several significant phenomena, including wide laser emission, spin electron reflectivity, and defect-induced magnetism. MgO nanostructures have a variety of applications, from spintronics to wastewater treatment, depending on their size and shape. Mg is sensitive material for hydrogen and forms MgH_2, so we used Mg/MgO as a sensor to sense hydrogen gas in the present work. Magnesium oxide thin films were synthesized by electrodeposition technique using magnesium nitrate salt. XRD results suggested that the deposited thin films have a face-centered cubic structure. X-ray photoelectron spectroscopy was used to detect the elemental composition and chemical state with the general electronic structure of the sample. The morphology and growth of deposited nanostructure with elemental mapping of the thin film were investigated by SEM-EDS. The UV-visible analysis shows the calculated band gap for MgO thin filmwas 4.16 eV which is in the ultraviolet region. The I-V characteristics have been studied to find out the effect of hydrogenation on the synthesized MgO nanostructure and the sensitivity responseof about 31%. It is quiteevident that MgO nanostructure may be used for gas sensing applications (such as H_2 gas).

Introduction

Nanostructure magnesium oxide thin films have drawn considerable attention because of their specific physical, chemical, and optical properties. Magnesium oxide, an insulating ionic simple oxide, crystallizes in bulk in the rock salt structure. The synthesized metal oxides with proper phase and structures have great interest in order to realize their specific properties that not only depend on their chemical composition but also on their shape,size, phase, crystal, and electronic structure as well as absorption ability, catalytic ability, surface reaction activity (Lan *et al.* 2011; Chatterjee *et al.* 2009; Bhatte *et al.* 2012). Since the discovery of carbon nanotubes, researchers have focused intensely on developing nanostructures made of other materials in a variety of domains (Huang *et al.* 2013; Yourdkhani and Caruntu 2011). Nano-cubes, nanorods, and nanoflowers are the most coveted types of nanostructures, in addition to nanoparticles and thin films.For many oxide systems, these kinds of nanostructures and their advantages are being examined (Wang *et al.* 2016; Weber *et al.* 2008). Magnesium oxide is a non-toxic, non-corrosive material that is rapidly utilized in composite materials for space flight, medicine, toxic waste treatment, and catalysis (Zou *et al.* 2008; Jia *et al.* 2013; Wang and Xue 2006). A variety of electrochemi-cal biosensors have recently been created employing nanoscale MgO material as a precise and sensitive tool for analytical application and diagnostic analysis (Ma *et al.* 2011; Li *et al.* 2009). Magnesium oxide has strong thermal conductivity as well as an excellent electrical insulator so valuable as thermocouples and heating systems components.

*Corresponding author's e-mail: clsaini52@gmail.com; clsaini52@uniraj.ac.in

MgO was known asa low-cost and environment-friendly material that has so many applications like bioresorbable materials that dissolve in biofluids (Huang, 2018), drug delivery (Ravaei *et al.* 2019), electrodes in pharmaceuticals and human fluids (Kairya *et al.* 2017), resistive switching (Guo *et al.* 2019), luminescence (Nikiforov *et al.* 2016), photo-catalytic properties (Demirci *et al.* 2015) and ultra-violet (UV) photodetector (Zhou *et al.* 2019). MgO nanostructures have also been reported to exhibit thermoluminescence (Abramishvili *et al.* 2011), radioluminescence (Skvortsova and Trinkler 2009), and electroluminescence (Benia *et al.* 2007). Thin metal oxide films that are electrically insulating are a crucial component of many different technologies, so magnesium oxide (MgO) has received a lot of attention for applicationssuch as spintronic devices since it has a material with a reasonably high dielectric constant. Under the influence of UV light, methyl orange, and methylene blue dyes were degraded using the photocatalytic activity of MgO nanoparticles (Mageshwari *et al.* 2013). Hydrogen storage properties of Mg/Ti bilayer thin films were reported (Jangid *et al.* 2021) at a different hydrogen pressure of 15 to 45 psi to realize the effect of hydrogenation. Hydrogen is the lightest element in the universe, which is typical to detect and magnesium is very sensitive to hydrogen in comparison to other metals. (Chawla *et al.* 2022). Although magnesium (Mg) is one of the better aspects for absorbing hydrogen, difficult to use this material for mobile applications due to its slow dynamics and need for high temperatures during dehydrogenation. Due to its extremely large reversible hydrogen capacity, magnesium hydride is particularly intriguing (Jangid *et al.* 2021). The present work reports the electrical behaviour and sensitivity of magnesium oxide (MgO) asa sensor to sense H_2 gas. In a similar work dip-coated CuO thin films were used to investigate the gas-sensing response of CO_2

vapor in air at room temperature and reported that the physical qualities that can be altered have a lot of potential for CO_2 gas-sensing applications. (Musa *et al.* 2021).

For the synthesis of thin films with nanostructures, an easy, affordable, and solution-based hybrid method is electro-deposition. MgO nanostructures have been grown successfully from an aqueous solution of magnesium nitrate $Mg(NO_3)_2$ using the electrodeposition method (Taleatu *et al.* 2014). The deposition procedure can be applied to a variety of conductive substrates, including polymers, semiconductors and ITO-coated glass. Indium tin oxide (ITO) is the most widely used substrate because of its outstanding transparency to visible light and high electric conductivity (Muchuweni *et al.* 2017). In the present work, magnesium oxide nanostructure thin film deposited by electrode position technique using magnesium nitrate solution. To synthesize MgO nanostructure, a variety of experimental procedures have been proposed, including reactive sputtering (Choi and Kim 2004), metal-organic molecular beam epitaxy (Niu *et al.* 2000), chemical vapor deposition (Carta *et al.* 2007), sol-gel (Zulkefle *et al.* 2011), and pulsed laser deposition (Kaneko *et al.* 2013).

Materials and methods

A conventional homemade two-electrode electrochemical bathsetup with labelled diagram shown in Fig. 1(b) was used in which graphite sheet was used as a counter electrode and ITO coated glass substrate as a working electrode. Both electrodes were introduced in the bath through two steel tubes. The electrolyte solution of 0.25 M concentration was prepared using magnesium nitrate $Mg(NO_3)_2$ salt. Before the deposition process, the ITO-coated glass substrate was extensively cleaned in an
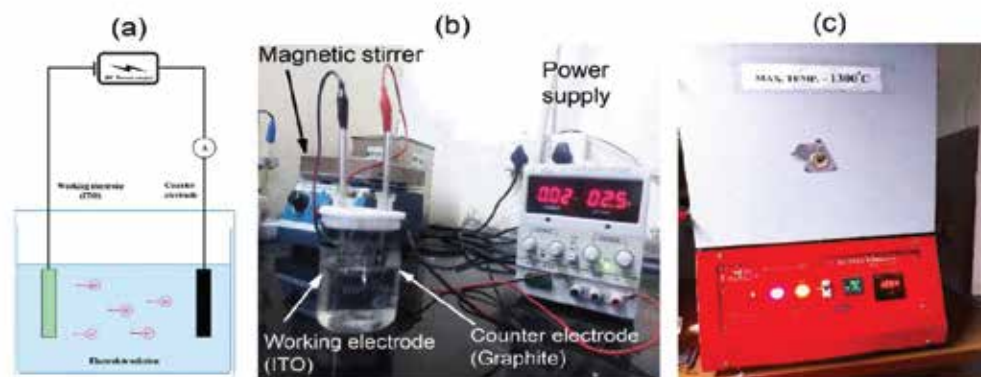

Fig. 1: (a) Schematic block diagram (b) Electrodeposition working setup and (c) furnace for heating

ultrasonic bath and rinsed with ultrapure water prior to the deposition in order to remove any surface impurities.
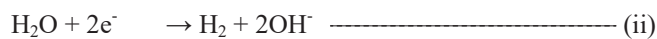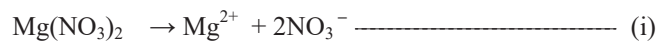
By applying a potential difference of 2.5 V at room temperature for 30 minutes by HTC power supply DC 3002, a thin layer of MgO nanostructures was deposited on ITO substrate. The deposited sample was dehydrated up to 350℃ at a heating rate of 10℃/min in a furnace shown in Fig. 1(c) and hold for 90 minutes and thencooled at natural/normal atmosphere conditions, finally, MgO nanostructure was formed.

Characterization of the nanostructure

Shimadzu UV-2600 UV-visible Spectrometer was used to analyze the optical characteristics, and Fourier Transform Infrared Spectrometer (FTIR) Bruker Alpha was used to collect data about various functional groups present in the samplein the range 4000–500 cm^{-1}. The structural and morphological characterization of the deposited nanostructure thin films was characterized by X-ray diffraction (XRD, Model: a Siemens D-5000 X-ray diffractometer) using Cu-K_α [1.54Å] radiation. The kinetic energy distribution of photoelectrons released from the specimen material was measured using X-ray photoemission spectroscopy (Model: Omicron ESCA (Electron Spectroscope for Chemical Analysis) Oxford Instrument Germany). In this model aluminium anode was used for samplesthat have energy 1486.7 eV. SEM (Model: JSM-7610F Plus & make: JEOL) was used to analyze the surface morphology and microstructure of deposited MgO nanostructures. The I-V characteristics for hydrogensensing were measured by using a Keithley Electrometer 6517A and a pressure-composition-isotherm (PCI) setupat vacuum (1 *10^{-3} mbar) and by introducing hydrogen (at 5 bar) in the stainless-steel chamber.

Results and discussion

Following equations (i-iv) show the overall chemical reaction for the deposition of MgO nanostructure thin film

$$Mg(NO_3)_2 \rightarrow Mg^{2+} + 2NO_3^{-} \text{------------------------} (i)$$

$$H_2O + 2e^{-} \rightarrow H_2 + 2OH^{-} \text{----------------------------} (ii)$$

$$Mg^{2+} + 2OH^{-} \rightarrow Mg(OH)_2 \text{------------------------------------}(iii)$$

Dehydration of $Mg(OH)_2$ produces MgO nanostructures onto ITO substrate.

$$Mg(OH)_2 \rightarrow MgO + H_2O \text{-------------------------------------}(iv)$$

using magnesium nitrate salt in aquas medium (Hashaikeh and Szpunar 2009).

X-ray diffraction (XRD) analysis

Diffraction measurement was carried out with an angular scanning range of (20° – 80°) to explore the nature of the material, purity, and crystallinity of the sample. Fig. 2 shows the XRD pattern of synthesized nanostructure thin films. In Fig. 2, spectrum (a) shows XRD pattern of theusedITO substrate, (b) shows the XRD pattern of thin film before annealing and (c) shows the XRD pattern of thin film after annealing. As discussed in equation (iii) and (iv) the XRD pattern represented by Fig. 2(b) for $Mg(OH)_2$ and Fig. 2(c) for MgO. The substrate peak marked by (*) is visible after post annealing at 350°C when conversion of $Mg(OH)_2$ into MgO nanostructure at ITO substrate (Alsultany *et al.* 2014).

$$D = \frac{0.9\lambda}{\beta \cos\theta} \text{---} (v)$$

Fig. 2(c) has distinctive sharp peaks correspond to (111), (200), (220) and (222) planes related to fcc structure (Cvetkovic *et al.* 2018). The sharp peaks illustrate that the synthesized nanostructure has a good crystalline nature. The Debye-Scherrer equation (Ashok *et al.* 2016) was used to compute the crystallite size D (nm).
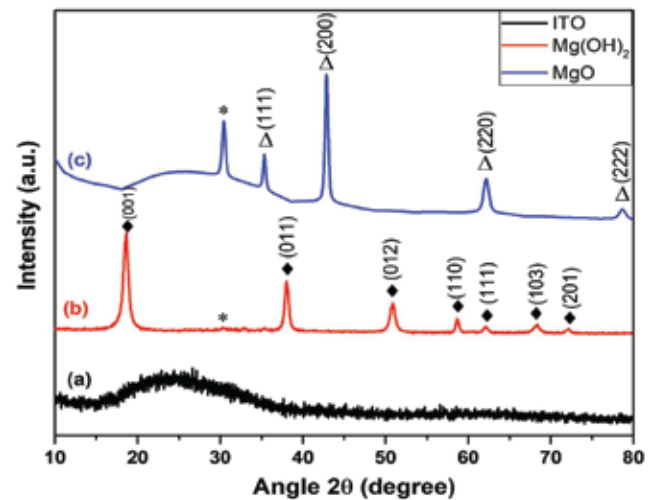

Fig. 2. XRD spectrum (a) bare ITO (b) synthesized $Mg(OH)_2$ and (c) MgO thin film

where λ, β, and 2θ were the wavelength of the incident X-ray beam (Cu K$_\alpha$ 1.54 Å), full width at half maximum (FWHM) in radian and Bragg's diffraction angle of the preferred orientation. The mean calculated crystalline size (D) for the deposited nanostructure was determined to be approximately 36 nm.

A surface-sensitive spectroscopic method (XPS) was used to determine the various elements present in a material (also known as its elemental composition), as well as their chemical state, general electronic structure, and density of their electronic states. The investigations about surface composition and chemical state of deposited MgO nano-

of the sample, the presence of carbon (C), oxygen (O), and magnesium (Mg) elements and no major contaminant can be seen which validate by the elemental signals received. Contamination of carbon was due to the environmental presence during the synthesis process which can be seen in Fig. 3a. The Mg 1s core level at 1302.8 eV is the peak with the highest intensity in the spectrum of deposited MgO nanostructure. The peak observed at 531.64 eV corresponds to O^{2-} in the lattice of MgO.

The core level spectra of Mg2p were also shown in fig. 3d, where a Gaussian peak of MgO at B.E. 50.91 eV was fitted
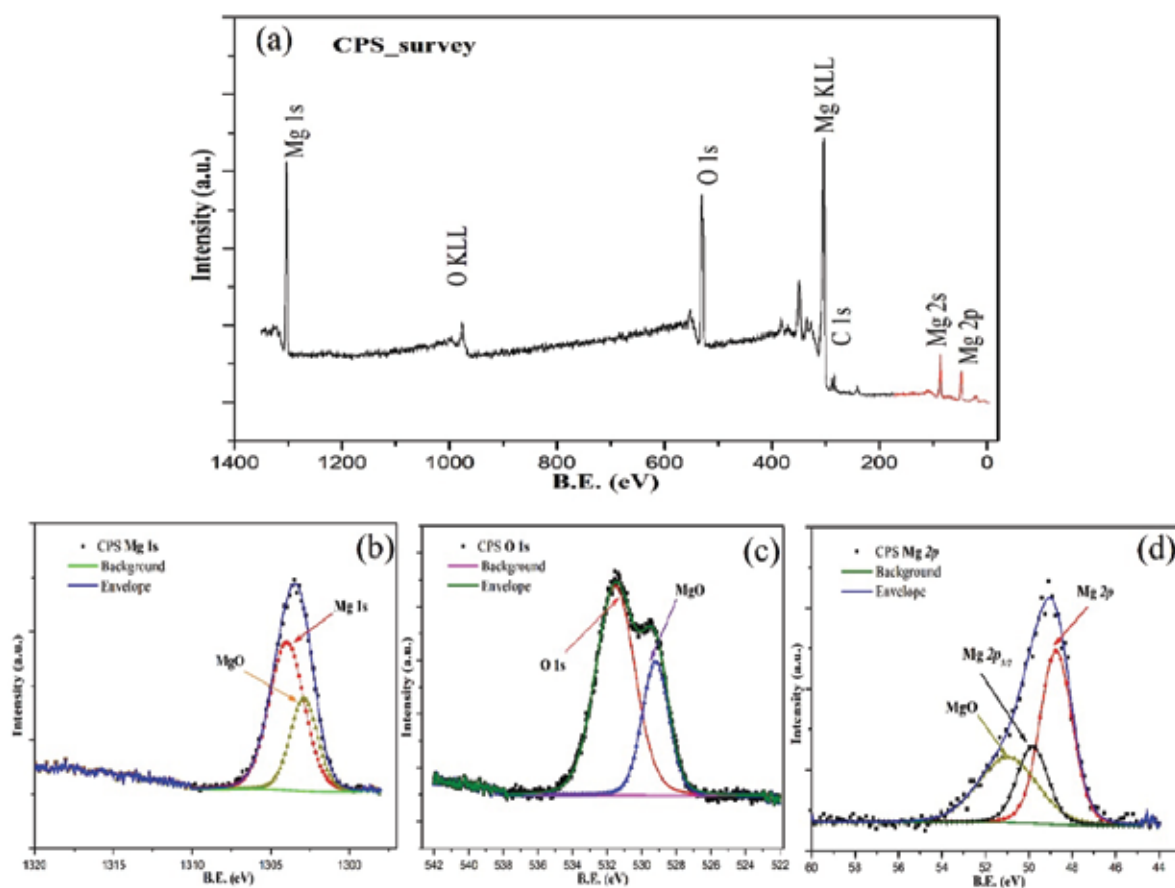

Fig. 3. (a) Survey scan of deposited MgO nanostructure and core level of (b) Mg 1s (c) O 1s (d) Mg 2p

structures using core-level light emission were reported and shown in Fig. 3. It was clear from the survey scan (Fig. 3a) that the deposited nanostructures were the MgO nanostructure during the synthesis process and no substantial pollutant was present in the sample. In the survey scan

using the CASA XPS software, and results indicate that the nanostructure of MgO was present with Mg lattice, which also confirms the existence in the core level spectra of Mg 1s (Fig. 3b) and O 1s (Fig. 3c) where MgO peak also present with lattice oxygen in the sample. The Mg 2p peak analysis in

Fig. 3d demonstrates that Mg remains in a single chemical state throughout the development process, and the characteristic B.E determines its oxidation.

The binding energy of all peaks related to elemental composition with the electronic state in the survey scan from Fig. 3(a) is tabulated as follows:

Table 1. B.E. for different elements available in MgO nanostructure thin film

Elemental composition	Binding Energy (eV)
Mg 1s	1302.8
O KLL	976.23
O 1s	531.64
Mg KLL	304.64
C 1s	285.41
Mg 2s	86.98
Mg 2p	48.21

Scanning electron micrograph (SEM) analysis

The SEM micrographs of the deposited MgO nanostructured thin films were obtained and shown in Fig. 4 together with the chemical elemental mapping. The inset table provides information about the elements which were found in the deposited nanostructure. The results indicate that the MgO nanostructure was synthesized with porous surface and deposited accurately by this method. As the number of porous was more on surface of deposited film than it would be easy for detecting the gas by increasing the amount of active area that is available for gas adsorption (Liu *et al.* 2014; Liu *et al.* 2016; Musa *et al.* 2021). The chemical compositions of the deposited nanostructure thin film on ITO substrate are also measured by EDX detector which is inbuilt into SEM. It is also evident that the nanostructure was adequately present in the form, which supports the XPS results.

UV-Visible Analysis

The absorption spectra of the synthesized magnesium oxide nanostructure thin films were obtained in the range of 200 and 800 nm using UV-visible spectrometer. Tauc's formula in equation (vi) was used to calculate the band gap of synthesized MgO nanostructure (Tauc *et al.* 1966)

$$(\alpha h v)^2 = C(h v - E_g) \text{ -- (vi)}$$

where α, *h*, *v*, *C* and E_g are the absorption coefficient, Plank's constant, frequency of the incident photon, a constant, and the direct transition band gap respectively. The UV-visible spectra were shown in Fig. 5, in which Fig. (a) indicates the absorbance spectrum (b) represents Tauc's plot to determine the optical band gap while Fig. (c) denotes the derivative of absorbance versus energy for verification of band gap and (d) transmittance spectrum for the deposited MgO
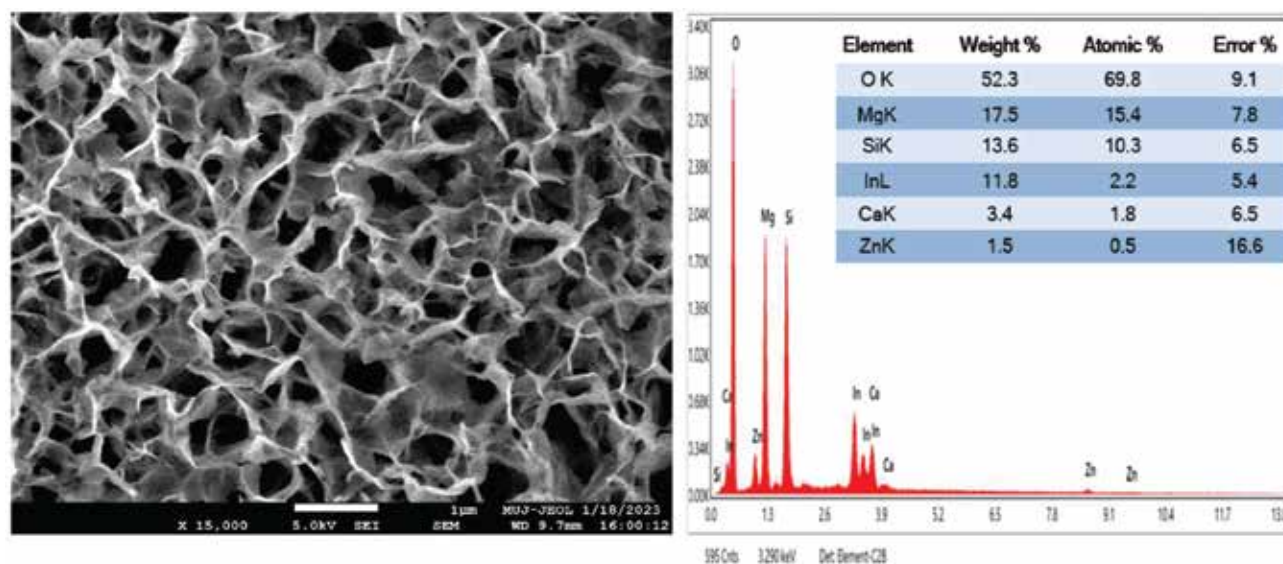

Element	Weight %	Atomic %	Error %
O K	52.3	69.8	9.1
MgK	17.5	15.4	7.8
SiK	13.6	10.3	6.5
InL	11.8	2.2	5.4
CaK	3.4	1.8	6.5
ZnK	1.5	0.5	16.6

Fig. 4. Micrograph of synthesized MgO with elemental mapping

nanostructure. The calculated band gap with the help of the above equation and extrapolation of the curve as shown in Fig. 5(b) was found about 4.16 eV, which is less than the band gap of bulk magnesium oxide (7.8 eV) as reported by many authors (Bilalbegovic *et al.* 2004; Guney *et al.* 2018; Egwunyenga *et al.* 2019; Baghezza, 2019). The band gap

rise in film thickness. Tlili *et al.* (2021) studied the variation of band gap from 4.01 to 4.08 eV for different molar concentrations (0.05, 0.1, 0.15, 0.2 $mol \cdot L^{-1}$) of Mg^{2+} ions by spray pyrolys is technique and reported that, as the molar concentration of Mg^{2+} increases, the optical band gap decreases.
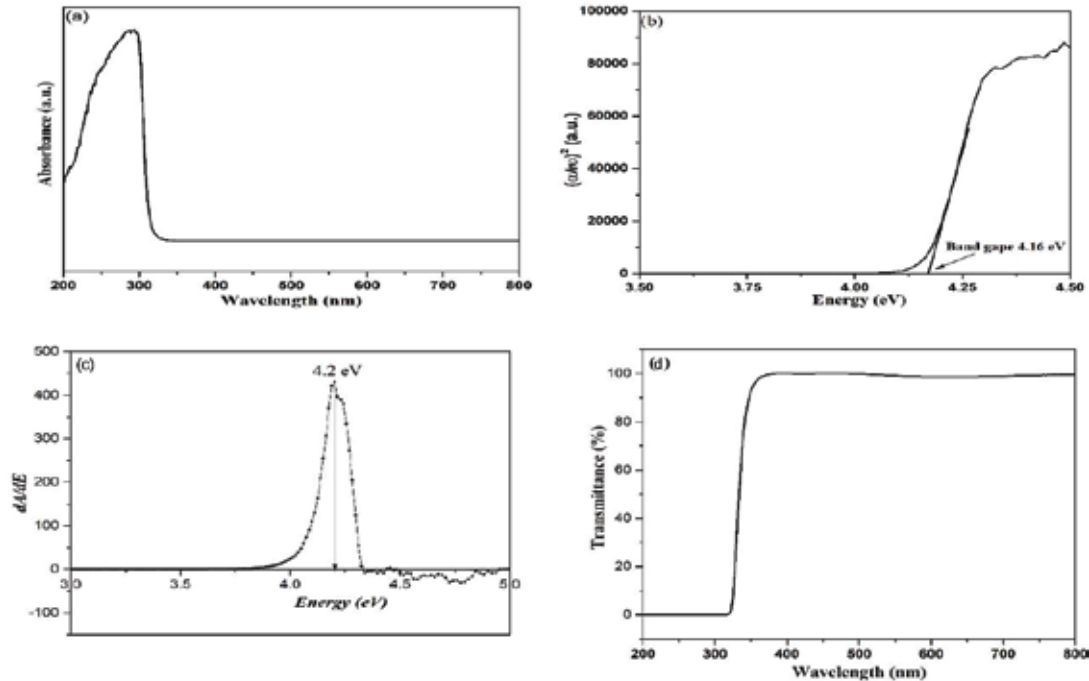

Fig. 5. UV-visible spectra of synthesized MgO thin film(a) Absorbance spectrum (b) Tauc's plot (c) derivative of absorbance versus energy (d) Transmittance spectrum

was also verified by the derivative versus energy curve which has a peak at 4.2 eV as shown in Fig. 5(c). The resultant curve was linear throughout a wide range of photon energy, showing that the deposited nanostructure was a direct transition material. The band gap of metal oxide nanostructure decreases due to presence of defect states, so these defectstates are responsible for the large difference in band gap energy. Both nanoparticles and nanostructures exhibit the same trend in band gap energy fluctuation however, nanostructures have a lower band gap energy than nanoparticles of the same size because of increased lattice strain and a larger surface to volume ratio (Abdullah *et al.* 2022). Guney and Iskenderoglu, (2018) found that the band gap of MgO nanostructures varied with thickness from 4.31 to 4.61 eV and that the band gaps were decreased as sample thickness increased. The reduction in band gap may be related to variations in the atomic distance with the
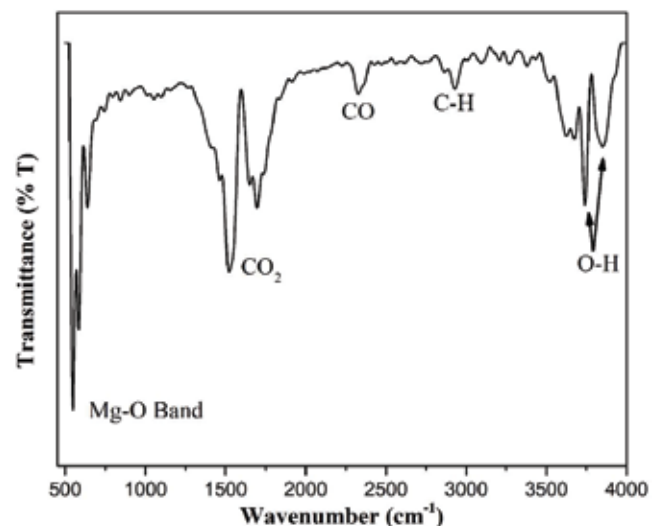

Fig. 6. FTIR spectra of synthesized MgO nanostructure

FTIR Analysis

FTIR spectroscopy was used to detect the existence of organic or inorganic constituents in the deposited nanostructure, which was connected to various functional groups associated with specific absorbance peaks in the spectra. The FTIR spectra of deposited MgO nanostructure thin film with transmission peaks ranging from 500 to 4000 cm^{-1} are shown in Fig. 6. The peak obtained at 545 cm^{-1} indicates the stretching vibration of MgO. As a result of the chemicals used during the synthesis process, the sample also contained additional functional groups at various peaks corresponding to CO_2, -CO, C-H and -OH, etc.

Electrical properties

The electrical properties such as current-voltage (I–V) characteristics were measuredin vacuum and with hydrogen gas by Keithley Electrometer 6517A in the range from -3 volt to 3 voltat room temperature. This study provides detailed information about the electronic effects in presence of hydrogen gas on deposited MgO nanostructure thin film.
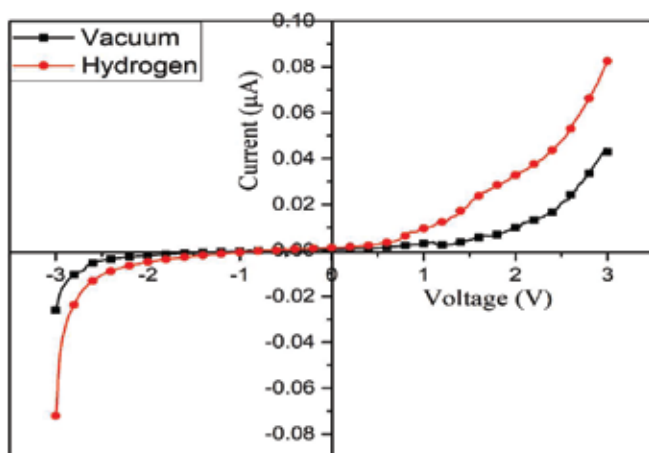

Fig. 7. Current-voltage characteristics of synthesized MgO nanostructure thin film (In vacuum and with Hydrogen)

The curve exhibits considerable nonlinearity compared to a thin MgO tunnel barrier. It can be seen from Fig. 7 that in presence of hydrogen gas, the conductivity increases in forward bias as well as in reverse bias, which can be explained as the charge shift from hydrogen to the film structure because hydrogen acts like a donor element. This property of MgO offers useful information about gas sensing applications like hydrogen gas and also can be employed as hydrogen storage materials. A similar study has been reported for Mg/Ti bilayer thin films (Jangid *et al.*

2021), Mg-Ni thin films (Jangid and Jangid, 2022) and for CdTe/Mn bilayer thin films (Nehra *et al.* 2009) that show the hydrogen storage properties of these bilayer thin films.

A stainless-steel sealed chamber containing the synthesized sample was usedto measurecurrent-voltage characteristics while exposed to H_2 gas in vacuum. The block diagram and PCI/PCT set up sown in Fig. 8. The resistance response of synthesized MgO thin film was converted into a sensitivity value using equation (vii) (Moumen *et al.* 2019; Musa *et al.* 2021).

$$\text{Response (\%)} = \frac{R_0 - R_g}{R_0} \times 100\ \% \quad\text{(vii)}$$

Where R_0 stands for the film's resistance in vacuum, and R_g for its resistance after being exposed to H_2 gas. Using equation (vii), the MgO nanostructure's sensitivity response to H_2 gas was estimated to be about 31%.
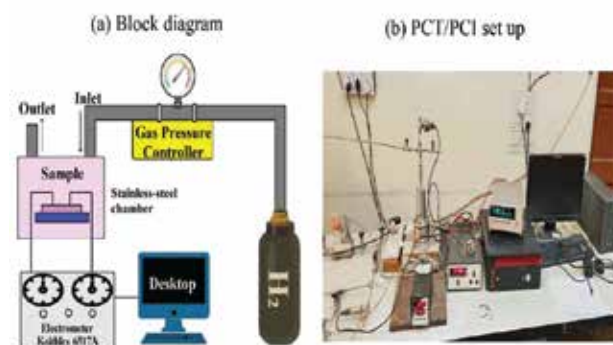

Fig. 8. Experimental gas sensitivity measurementsetup (a) Schematic block diagram (b) PCT/PCI setup

Conclusion

The MgO nanostructure thin film was synthesized on ITO-coated glass substrate at room temperature by a simplified electrodeposition method using aqueous solution of magnesium nitrate and investigated by different characterization techniques. A cubic structure of MgO with a predicted crystalline size of about 36 nm was calculated by XRD investigation. The SEM-EDX image confirms the porous structure, adherent to the substrate and atomic % of available elements in the deposited MgO nanostructure thin films. The elemental composition and chemical states with binding energy were obtained using XPS. The UV-visible analysis confirmed the optical band gap of the deposited nanostructure was ~ 4.16 eV. The I-V characteristics of deposited nanostructure suggest the partial semiconductor nature and the

conductivity increases in presence of hydrogen. The sensitivity response of deposited nanostructure was approximately 31% on exposure to H_2 gas. The deposited MgO nanostructures provide useful information about gas sensing applications such as hydrogen gas and also can be employed as hydrogen storage materials. The ultrafine nanostructures (such as QDs etc.) provide a large and sensitive surface area for a promising solution to decrease the operating temperature for metal oxide semiconductor-based gas sensors (Liu *et al.* 2014; Liu *et al.* 2016). Their high surface energy allows for the absorption of gas molecules even at room temperature for the sensing application.

Acknowledgement

References

Abdullah BJ (2022), Size effect of band gap in semicon-ductor nanocrystals and nanostructures from density functional theory within HSE06, *Materials Science in Semiconductor Processing*, **137**: 106214. DOI: 10.1016/j.mssp.2021.106214.

Abramishvili M, Akhvlediani Z, Galustashvili M, Dekanozishvili G, Kalabegishvili T, Kvatchadze V and Tavkhelidze V (2011), Peculiarities of radiation effects in MgO: Mn^{2+} crystals, *Journalof Modern Physics* **2**: 841–844. DOI:10.4236/jmp.2011.28099.

Alsultany FH, Ahmed NM and Matjafri MZ (2014), Effects of CW CO_2 laser annealing on indium tin oxide thin films characteristics, *Soft Nanoscience Letters* **4**(04)**:** 83. DOI: 10.4236/snl.2014.44012.

Ashok C, Rao KV, Chakra CS and Rao KG (2016), MgO nanoparticles prepared by microwave-irradiation technique and its seed germination application, *Nano Trends: A Journal of Nanotechnology and its application* **18**: 10-17. DOI: 10.3390/nano11113076

Baghezza Mohammad (2019), Optical and electrical proper-ties of MgO thin films. Khider University, M. L. B. M. M, http://a rchives. univ- biskra. dz/ handle/ 123456 789/13780.

Bilalbegovic, G. (2004), Structural and electronic properties of MgO nanotube clusters, *Physical Review B* **70**(4): 045407. DOI: 10.1103/PhysRevB.70.045407.

Benia HM, Lin X, Gao HJ, Nilius L and Freund HJ (2007), Nucleation and growth of gold on MgO thin films: A combined STM and luminescence study, *Journal of Physical Chemistry C***111**: 10528-10533. DOI:10. 1021/jp0726891

Bhatte KD, Sawant DN, Deshmukh KM, Bhanage BM, Rusdi R, Kamarudin N, Llanos M and Lopez-Salinas (2012), Additive free microwave assisted synthesis of nanocrystalline $Mg(OH)_2$ and MgO, *The Lancet* **10**: 384-387. DOI: 10.1016/j.partic.2011.05.004

Carta G, Habra N El, Crociani L, Rossetto G, Zanella P, Paolucci G, Barreca D and Tondello E (2007), CVD of MgO Thin Films from Bis(methylcyclopentadienyl) Magnesium, *Chemical Vapor Deposition* **13**(4): 185-189. DOI:10.1002/cvde.200606574

Chatterjee S, Gohil S, Chalke Band Ayyub P (2009), Optimi-zation of the morphology of ZnO nanorods grown by an electrochemical process, *Journalof Nanoscience and Nanotechnology* **9**(8): 4792- 4796. DOI: 10. 1166/jnn.2009.1094

Chawla K, Yadav DK, Bajpai A, Kumar S, Jain IP and Lal C (2022), Effect of $PdCl_2$ catalyst on the hydrogenation properties and sorption kinetics of Mg, *International Journal of Hydrogen energy* **51**: 101981. DOI: 10.1016/ j.seta.2022.101981

Choi YW and Kim J (2004), Reactive sputtering of magne-sium oxide thin film for plasma display panel applica-tions, *Thin Solid Films* **460**: 295-299. DOI: 10.5370/-JEET.2006.1.1.110

Cvetkovic VS, Vukicevic NM, Nikolic ND, Brankovic G, Barudzija TS and Jovicevic JN (2018), Formation of needle-like and honeycomb-like magnesium oxide/hy-droxide structures by electrodeposition from magne-sium nitrate melts. *Electrochimica Acta* **268**: 494-502. DOI: 10.1016/j.electacta.2018.02.121.

Demirci SO, Zturk B, Yildirim S, Bakal F, Erol M, Sancakog-lu O, Yigit R, Celik RE and Batar T (2015), Synthesis and comparison of the photocatalytic activities of flame spray pyrolysis and sol-gel derived magnesium oxide nano-scale particles, *Materials Science in Semiconductor Processing* **34**: 154-161. DOI: 10.1016/j.mssp. 2015.02.029

Egwunyenga NJ, Ezenwa IA and Ezenwaka LN (2019), Optical properties of Electrodeposited Magnesium Oxide Thin Films, *COOU Journal of Physical Sciences* **1**(2): 11-18.https:// coou.edu.ng/ journals/ cjops/c-jps1219002.pdf.

Guo Y, Song Q and Yan H (2019), The influence of interaction between oxygen vacancies on set process in resistive switching: a case of MgO,*AIP Advances* **9**: 055230(1-7). DOI:10.1063/1.5092690.

Guney H and Iskenderoglu D (2018), Synthesis of MgO thin films grown by SILAR technique, *Ceramics International* **44**(7): 7788-7793. DOI: 10.1016/j.ceramint.2018.01.210

Hashaikeh R and Szpunar JA (2009), Electrolytic processing of MgO coatings, Conference Series, International Conference on Advanced Structural and Functional Materials Design, *Journal of Physics* **165**: 012008:1-4. DOI:10.1088/1742-6596/165/1/012008

Huang X (2018), Materials and applications of bioresorbable electronics, *Journalof Semiconductors* **39**: 011003(1-10). DOI: 10.1088/1674-4926/39/1/011003

Huang X, Gonzalez-Rodriguez R, Rich R, Gryczynski Z and Coffer JL (2013), Fabrication and size dependent properties of porous silicon nanotube arrays, *Chem-Comm (RSC Publishing)* **49**: 5760-5762. DOI: 10.1039/C3CC41913D

Jangid MK, Sharma SS, Mathur D and Sharma YC (2021), Optical, electrical and structural study of Mg/Ti bilayer thin film for hydrogen storage applications, *Materials Letters: X* **10**: 100076(1-4). DOI: 10.1016/j.mlblux-.2021.100076

Jangid MK and Jangid SK (2022), Structural, Electrical and Optical Properties of Mg-Ni Thin Films for Hydrogen Storage Applications, *Trends in Science* **19**(23): 2067(1-8). DOI:10.48048/tis.2022.2067

Jia Y, Luo T, Yu XY, Sun B, Liu JH and Huang XJ (2013), A facile template free solution approach for the synthesis of dypingite nanowires and subsequent decomposition to nanoporous MgO nanowires with excellent arsenate adsorption properties, *RSC Advances* **3:** 5430-5437. DOI: 10.1039/c3ra23340e.

Kaneko S, Ito T, Soga M, Motoizumi Y, Yasui M, Hirabayashi Y, Ozawa T and Yoshimoto M (2013), Growth of Nanocubic MgO on Silicon Substrate by Pulsed Laser Deposition, *Japanese Journal of Applied Physics* **52**(15): 01AN02(1-3). DOI: 10.7567/JJAP.52.01AN02

Khairya M, Khorshed AA, Rashwan FA, Salah GA, Abdel-Wadood HM and Banksd CE (2017), Simultaneous voltametric determination of antihypertensive drugs nifedipine and atenolol utilizing MgO nano-platelet modified screen-printed electrodes in pharmaceuticals and human fluids, *Sensorand Actuators B: Chemical* **252**: 1045-1054. DOI: 10.1016/ j.snb.2017.06.105

Lan X, Zhang JY, Gao H and Wang TM (2011), Morphology-controlled hydrothermal synthesis and growth mechanism of microcrystal Cu_2O, *Crystal Engineering Communication (Royal Society of Chemistry)* **13**: 630-636. DOI: 10.1039/C0CE00232A.

Li CF, Ho WH and Yen SK (2009), Effects of Applied Voltage on Morphology and Crystal Orientation of $Mg(OH)_2$ Coating on Pt by Electrochemical Synthesis, *Journal of Electrochemistry Society* **156**: E29-E34. DOI: 10.1149/1.3032174.

Liu H, Li M, Voznyy O, Hu L, Fu Q, Zhou D, Sargent EH, Tang J and Xia Z (2014), Physically Flexible, Rapid-Response Gas Sensor Based on Colloidal Quantum Dot Solids, *Advanced Materials* **26**: 2718-2724. DOI: 10.1002/adma.201304366

Liu H, Zhang W, Yu H, Gao L, Song Z, Xu S, Li M, Wang Y, Song H and Tang J (2016), Solution-Processed Gas Sensors Employing SnO_2 Quantum Dot/MWCNT Nanocomposites, *ACS Applied Materials & Interfaces* **8**: 840-846. DOI: 10.1021/acsami.5b10188

Ma J, Chen CZ, Wang DG and Hu JH (2011), Synthesis characterization and in vitro bioactivity of magnesium-doped sol-gel glass and glass-ceramics, *Ceramic International* **37**: 1637-1644. DOI: 10.1016/j.ceramint.2011.01.043

Mageshwari K, Mali SS, Sathyamoorthy R and Patil PS (2013), Template-free synthesis of MgO nanoparticles for effective photocatalytic applications, *Powder Technology* **249**: 456-462. DOI: 10.1016/j.powtec.2013.09.016.

Moumen A, Hartiti B, Comini E, Arachchige HMM, Fadili S and Thevenin P (2019), Preparation and characterization of nanostructured CuO thin films using spray pyrolysis technique, *Superlattices and Microstructures* **127**: 2-10. DOI: 10.1016/j.spmi.2018.06.061

Muchuweni E, Sathiaraj TS and Nyakotyo H (2017), Synthesis and characterization of zinc oxide thin films for optoelectronic applications, *Heliyon* **3**(4): e00285(1-18). DOI: 10.1016/j.heliyon. 2017.e00285

Musa AMM, Farhad SFU, Gafur MA and Jamil ATMK (2021), Effects of withdrawal speed on the structural, morphological, electrical, and optical properties of CuO thin films synthesized by dip-coating for CO_2 gas sensing, *AIP Advances* **11**(11): 115004. DOI: 10.1063/5.0060471

Nehra SP, Jangid MK, Kumar A, Singh M and Vijay YK (2009), Role of hydrogen in electrical and structural characteristics of bilayer CdTe/Mn diluted magnetic semiconductor thin films, *International Journal of Hydrogen Energy* **34**(17): 7306-7310. DOI: 10.1016/j.ijhydene.2009.06.054

Nikiforov SV, Kortov VS and Petrov MO (2016), Luminescent and dosimetric properties of ultrafine magnesium oxide ceramics after high dose irradiation, *Radiation-Measurements* **90**: 252-256. DOI: 10.1016/j.radmeas.2015.12.018

Niu F, Hoerman BH and Wessels BW (2000), Metalorganic molecular beam epitaxy of magnesium oxide on silicon, *MRS Online Proceedings Library* **619**: 149-154. DOI: 10.1557/PROC-619-149.

Ravaei I, Haghighat M and Azami SM (2019), A DFT, AIM and NBO study of isoniazid drug delivery by MgO nanocage, *Applied Surface Science* **469**: 103-112. DOI: 10.1016/j. apsusc.2018.11.005

Shinji Y, Taro N, Akio F, Yoshishige S and Koji A (2004), Giant room-temperature magnetoresistance in single-crystal Fe/MgO/Fe magnetic tunnel junctions, *Nature Materials* **3**: 868-871. DOI:10.1038/nmat1257

Skvortsova V and Trinkler L (2009), Luminescence of impurity and radiation defects in magnesium oxide irradiated by fast neutrons, *Physics Procedia* **2**: 567-570. DOI: 10.1016/j. phpro.2009.07.042

Taleatu BA, Omotoso E, Lal C, Makinde WO, Ogundele KT, Ajenifuja E, Lasisi AR, Eleruja MA and Mola GT (2014), XPS and some surface characterizations of electrodeposited MgO nanostructure, *Surfaceand Interface Analysis* **46**: 372-377. DOI: 10.1002/sia.5425

Tauc J, Grigorovici R and Vancu A (1966), Optical Properties and Electronic Structure of Amorphous Germanium, *Basic Solid-State Physics* **15**: 627-637. DOI: 10.1002/pssb.19660150224.

Tlili M, Nefzi C, Alhalaili B, Bouzidi C, AjiliL, Jebbari N and Turki Kamoun N (2021), Synthesis and characterization of MgO thin films obtained by spray technique for optoelectronic applications, *Nanomaterials* **11**(11)**:** 3076 (1-15). DOI: 10.3390/nano11113076.

Wang X, Feng J, Bai Y, Zhang Q and Yin Y (2016), Synthesis, properties, and applications of hollow micro-/nanostructures, *Chemical Reviews* **116**: 10983-11060. DOI: 10.1021/ acs.chemrev.5b00731

Wang X and Xue D (2006), Direct observation of the shape evolution of MgO whiskers in a solution system, *MaterialsLetters* **60**: 3160-3164. DOI: 10.1016/j.matlet.2006.02.066

Weber J, Singhal R, Zekri S and Kumar A (2008), One-dimensional nanostructures: fabrication, characterisation and applications, *International Materials Review* **53**(4): 235-255. DOI: 10.1179/174328008X348183

Yourdkhani A and Caruntu G (2011), Highly ordered transition metal ferrite nanotube arrays synthesized by template-assisted liquid phase deposition, *Journal of Material Chemistry* **21**: 7145-7153. DOI: 10.1039/C0-JM04441E

Zhou C, Ali Q, Chen X, Gao X, Liu K and Shen D (2019), Ultraviolet photodetectors based on wide bandgap oxide semiconductor films, *Chinese Physics B* **28**: 048503. DOI: 10.1088/1674-1056/28/4/048503

Zou G, Chen W, Liu R and Xu Z (2008), Morphology-tunable synthesis and characterizations of $Mg(OH)_2$ films via a cathodic electrochemical process, *Materials Chemistry and Physics* **107**: 85-90. DOI: 10.1016/j.matchemphys. 2007.06.046

Zulkefle H, Ismail LN, Bakar RA and Mahmood MR (2011), Molar concentration effect on MgO thin films properties, *In Proceedings of the IEEE Symposium on Industrial Electronics and Applications, Langkawi, Malaysia*, pp 468-471. DOI: 10.1109/ISIEA.2011.6108754.